J. LARJO*,✉
H. KOIVIKKO
K. LAHTONEN
R. HERNBERG

Two-dimensional atomic hydrogen concentration maps in hot-filament diamond-deposition environment

Tampere University of Technology, Optics Laboratory, P.O. Box 692, 33101 Tampere, Finland

ABSTRACT This paper reports the two-dimensional mapping of atomic hydrogen concentration with two-photon excited laser induced fluorescence in a multi-wire grid hot-filament chemical vapor deposition reactor. The measurements were made in a diamond film deposition environment under different filament temperatures and wire configurations. The measurement was calibrated with a titration reaction using NO_2 as a titrant. The kinetic gas temperature in the reactor was measured from the Doppler broadening of the Lyman-β transition excited in the fluorescence. The filament temperature was found to have a significant effect on atomic hydrogen production and transfer to the substrate. The axial concentration distributions were compared to a one-dimensional kinetic gas–surface chemistry model with good agreement. The model produced a reasonable estimate for the bulk diamond film growth rate.

PACS 32.50; 47.70

1 Introduction

The influence of atomic H on the growth process of a diamond film in a chemical vapor deposition (CVD) environment is well understood [1, 2]. H atoms participate in the growth both in the gas phase and on the substrate surface, generating the growth precursors and activating the surface for growth radical attachment. Atomic H is a main target for gas-phase diagnostics in diamond CVD; the measurement has been implemented using different techniques in various environments [3–8, 13].

Due to its experimental simplicity and low cost of operation, hot-filament CVD is one of the most popular methods in diamond-film growth. With this technique, the filament temperature T_F must be over 2000 K to achieve sufficient hydrogen dissociation for diamond-film growth. Atomic H concentration, and consequently the film growth rate and purity, increases substantially when increasing T_F. In our earlier work, we have reported growth rates in the order of 10 µm/h with T_F at 3100 K [9]. The high-temperature value is typically attained by using a compound filament material such as

WC or TaC. It is difficult to maintain uniform and stable filament conditions in the reactor over a large substrate area during long-term operation, due to the filament deformations and changes in filament radiative properties.

In this paper we present experimental H atom concentration measurements acquired with a two-dimensional laser-induced fluorescence (LIF) diagnostic system in a hot-filament CVD reactor. Results under different filament grid sizes and temperatures are presented. The LIF concentration measurement is calibrated using a NO_2 titration technique. A one-dimensional gas-phase and surface kinetic chemistry model was built to verify the consistency of the results.

2 Experimental

The reactor and diagnostic systems used in this work have been presented in detail previously [10, 13]. Briefly, the reactor is a grid-type TaC filament reactor, with 40-mbar operation pressure. In this reactor, the water-cooled Si substrate resides above the filament grid at approximately 7-mm distance. The substrate temperature T_S was held approximately at 900 °C. In this configuration, it is not necessary to move the brittle carburized filament in order to disassemble the substrate holder between operations. As the externally cooled substrate holder is above the heated filament in this case, the flow patterns caused by natural convection will be different from the more usual filament-above-substrate design. Thus, mass transfer by natural convection is challenging to analyze with this configuration; fortunately the hot-filament CVD process is largely dominated by diffusive mass transfer [11]. Nevertheless, it is possible that the flow patterns change significantly under different operation parameters, such as T_S, T_F and the number of wires in the filament. Convective heat transfer from the filament to the substrate will be affected as well, but radiative heat transfer will probably prevail, at least with high values of T_F.

We reduced the deformation of the filament during the carburization and operation stages by constructing a constant-tension filament-support structure (Fig. 1). This design attempts to counter the effects of thermal expansion and filament volume change during the carburization process. By visual inspection, the filament geometry was well preserved with this setup compared to the constant-length structure used

✉ Fax: +358-3/3115-2090, E-mail: jussi.larjo@oseir.com
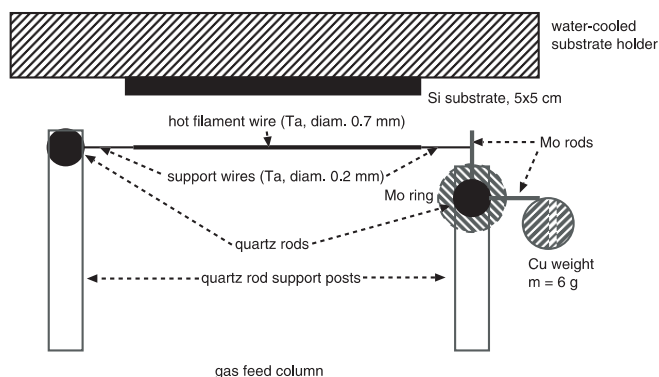*Present address*: Oseir Oy, Hermian Katu 6A, 33720 Tampere, Finland

FIGURE 1   The filament-support structure

earlier. The new structure did not substantially improve the filament durability against thermal and mechanical shocks.

The diagnostic system consists of a Nd:YAG-pumped dye laser operating at 205-nm wavelength, an optical system controlling beam focusing and vertical alignment and an intensified charge-coupled device (CCD)-type video camera detector. The laser-induced fluorescence excitation scheme is two-photon excitation of the H atom L_β transition with subsequent monitoring of fluorescence at the H_α wavelength of 656.6 nm. This scheme is frequently used in LIF of H atoms; it exhibits the highest sensitivity of all available multi-photon excitation schemes and has a good linearity between the H atom concentration and the fluorescence signal level, provided that precautions are taken with the laser pulse energy level to avoid effects like photodissociation and stimulated emission [12]. The gas mixture in the growth experiment was H_2/CH_4 in 98%/2% mixture.

The LIF measurement was calibrated by titration with NO_2, with a setup similar to the one described in detail in [3]. The H atom source was a custom-made microwave plasma reactor. The gas mixture of H_2 (5%) and He was partially dissociated in the reactor, mixed with a dilute mixture of NO_2 in He and led to the measurement volume. The LIF signal was measured as a function of the amount of NO_2 in the mixture, and the original H atom concentration in the flow at the measurement point could be determined from this titration curve.

In addition, one needs to provide a calibration factor C that can be used to provide the H atom concentration in the hot-filament environment:

$$[H]_M = C \frac{S_M}{S_C} [H]_C, \tag{1}$$

where S_C and $[H]_C$ are the LIF signal intensity and the H atom concentration during the calibration and S_M and $[H]_M$ the same during the actual measurement. The calibration-factor value depends strongly on numerous individual factors, like the gas-mixture composition, pressure and temperature and the laser-beam profile, and cannot be directly compared with the other findings in the literature. In our case, the numerical value of the factor was $C \approx 14$ in the input gas mixture, with a weak dependence on the gas temperature.

It was found that the dye laser alignment had a strong effect on the signal magnitude, presumably due to changes in the 205-nm beam-intensity profile. Care was taken in order not to re-align the dye laser optics between the calibration

and measurement procedures. This was not possible in long-term operation, so the calibration was repeated with each filament configuration. Thus, the uncalibrated signal levels are not comparable between filament configurations.

The main measurement parameters were the number of parallel wires in the filament grid and the filament temperature, as measured by a two-color optical pyrometer. The maximum filament temperature T_F attainable with ease in this reactor was 2600 °C. Above this point, breakage of the filament was not easily avoided in long-term operation. Also, the background radiation induced excessive CCD blooming that saturated the detector in the proximity of the filament area. Moreover, even small drifts in T_F caused substantial variation in the background intensity. For these reasons, the complete temperature maps presented below were measured with T_F at 2600 °C. We found that the laser beam access windows developed soot quite rapidly at the laser beam entry point with higher CH_4 feed rates. Measuring one complete map took approximately 10 min with manual alignment of the beam; the adjustment and settling between different filament temperatures took at least 5 min.

3   Results and discussion

3.1   *Two-dimensional LIF diagnostics*

Figure 2 shows the typical behavior of the measured fluorescence signal maps with 1, 3 and 5 filament wires. The original Ta wire thickness was 0.5 mm and the distance between different wires 5 mm in all measurements. In these and all following figures, x denotes the lateral distance from the substrate centerline, and z denotes the vertical distance below the substrate. It is seen that the 1-wire case exhibits almost radial symmetry close around the filament, and multi-wire cases have correspondingly broader laterally uniform signal maps around the system symmetry axis. In the 5-wire case, this area extends all over the substrate width of 28 mm. The effect of the substrate is seen close to the z-axis origin, acting as an H atom sink in the otherwise smoothly decreasing signal map structure. The substrate temperature T_S was approximately 900 °C in all measurements.

The features of the signal maps suggest that the growth conditions are spatially uniform in the 5-wire case. In the other cases, the growth at the substrate edges is suppressed due to the reduced H transfer rate, as seen from the signal vertical gradients. The quantitative H concentration maps and diffusive mass transfer rate profiles could be calculated using an accurate gas-temperature map, which is beyond the scope of this work.

Quantitative analysis was made on the axial one-dimensional profiles. We constructed the axial gas temperature profile by interpolation, using the measured values of T_F and T_S as reference points, after the experimental profiles measured earlier in lower filament temperatures. The interpolation models were derived from earlier works by Meier et al. [3], who used a theoretical model by Langmuir and Blodgett, and Connelly et al. [6], who verified their estimates using a coherent anti-Stokes Raman technique to determine an experimental T profile in the gas layer. In both references, the gas-temperature change was several hundred kelvins in submillimeter layers at
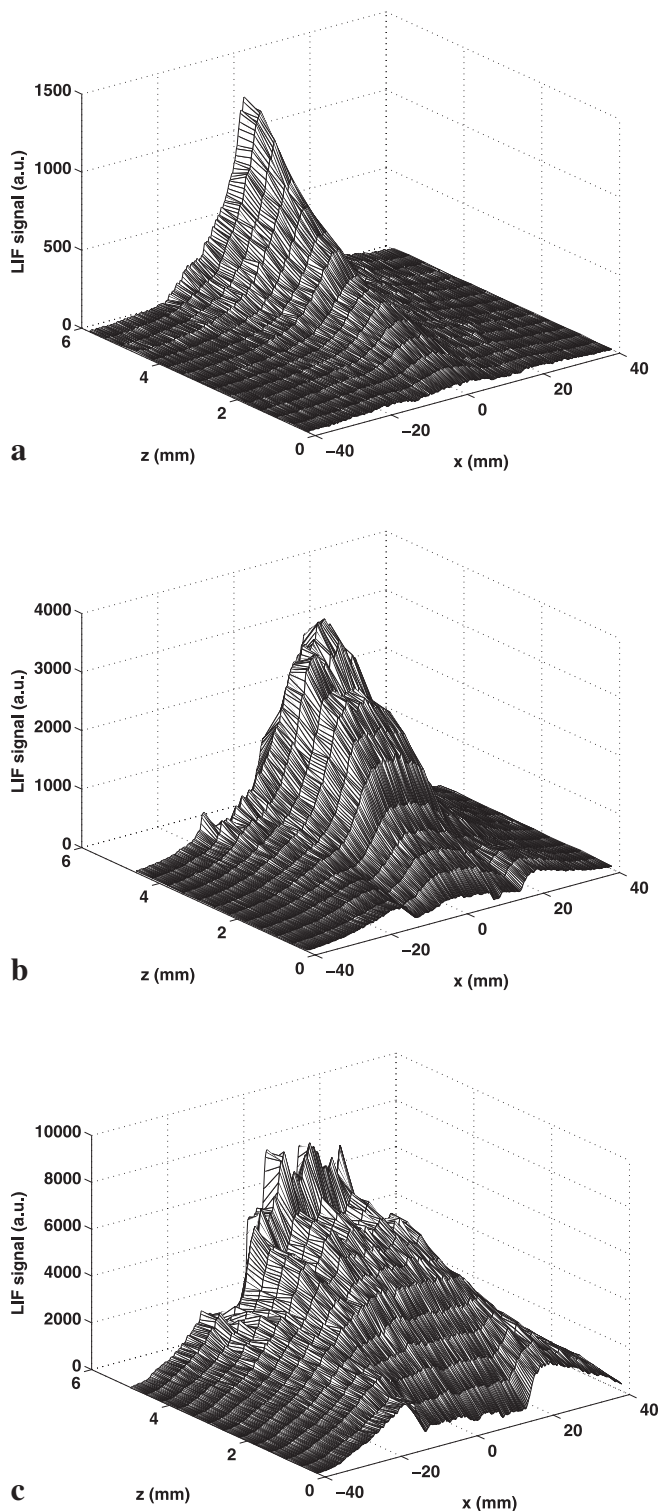
a

b

c

FIGURE 2 Measured two-dimensional LIF signal maps. *Top*: 1-wire; *middle*: 3-wire; *bottom*: 5-wire

both substrate and filament surfaces. Between these layers the temperature profile was linear.

To verify the validity of this approach, the L_β excitation line profile was measured using the LIF diagnostic system, by tuning the dye laser over the transition line and measuring the fluorescence intensity as a function of the wave number. The profile measurement resolution was $0.14\,\mathrm{cm}^{-1}$. This

measurement was only performed in the 5-wire configuration, under T_F of $2600\,^\circ\mathrm{C}$, at two points. The measured line profiles made an excellent Gaussian fit ($r^2 > 0.99$), with calculated Doppler gas temperatures at $2660 \pm 300\,^\circ\mathrm{C}$ at $z = 5.6$ mm and $1630 \pm 130\,^\circ\mathrm{C}$ at $z = 3.2$ mm. These results suggest that the transition is essentially Doppler-broadened. Most other relevant broadening mechanisms, like Stark or pressure broadening, contribute to a Lorentzian line profile as a first approxi-
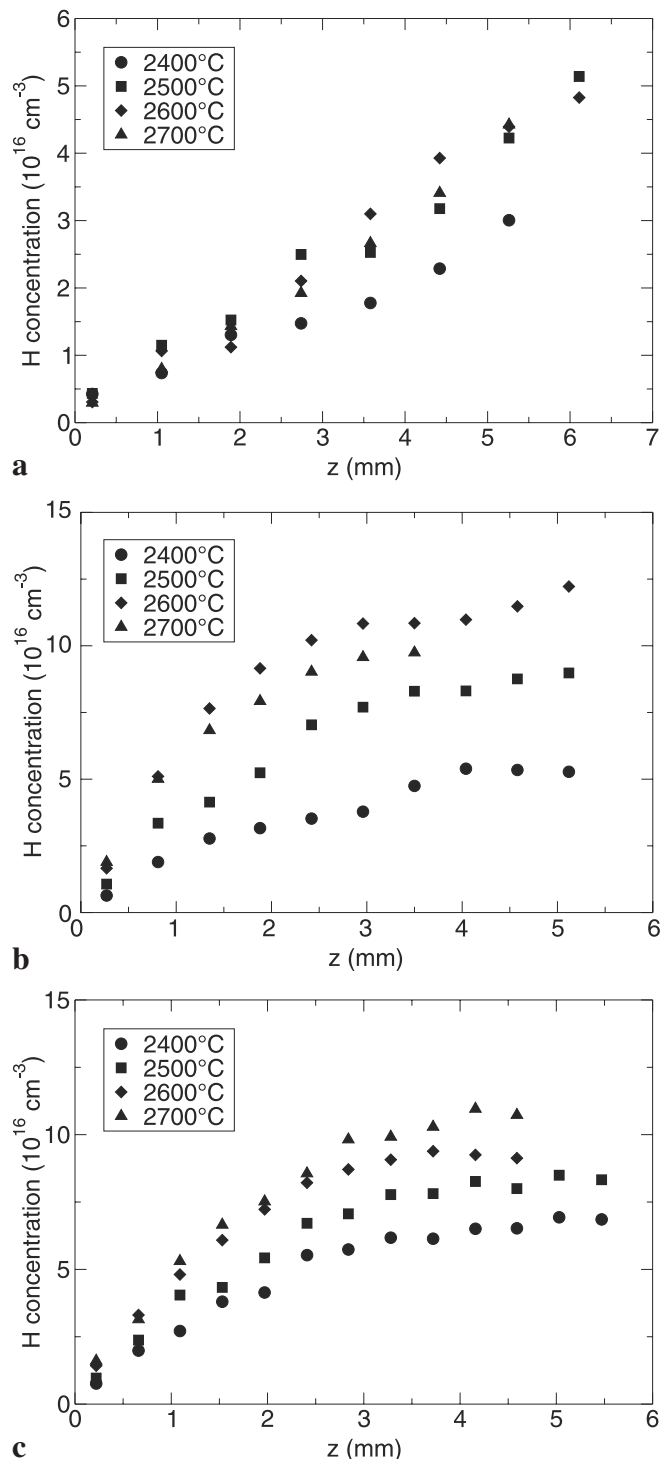

a

b

c

FIGURE 3 Calibrated axial H atom concentration profiles. *Top*: 1-wire; *middle*: 3-wire; *bottom*: 5-wire

mation, leading to a Voigt-type actual line profile when their influence is significant.

The vertical H concentration profiles at the symmetry axis for each filament configuration are displayed in Fig. 3 under different values of T_F. The dissociation close to the filament was found to be large enough to significantly lower the H_2 mole fraction, which in turn caused a strong decrement in C close to the filament. Therefore the presented absolute concentration profiles were adjusted using an iterative calculation similar to the one used in our thermal plasma CVD work [13]. In short, C was first re-calculated using the reduced H_2 mole fraction for each point in the profile. A new H atom concentration profile was obtained using the C profile, which again led to an adjustment in the H_2 mole fraction. This procedure was repeated until the difference between two successive H atom concentration profiles was less than 5%.

Generally, the results indicate that increasing the number of filaments produces significantly higher H atom concentrations. The reason for this is probably the improved atom production with increased filament surface area. As the gas-phase recombination is minimal in these conditions, the diffusive mass transfer is strong enough to considerably elevate the H concentration at the surface. Increasing T_F generally has the same effect. In the 3-wire case, at $T_F = 2700\,°C$ there is a notable discrepancy from this behavior. The probable explanation is that the filament broke down right after this experiment. So, H atom production was reduced due to the degradation of the filament surface at the end of its lifetime.

In our earlier work in this environment [10], we observed a decreasing LIF signal when approaching the filament, a probably nonphysical result that was not repeated in this setting. In the measurements presented in this paper, extreme care was taken so that the large solid angle of the detector was not partially obstructed by the support structures at any point included in the presented results. The partial screening effect of the substrate holder at low values of z was also accounted for in the presented axial profiles. This was amended by calculating the appropriate correction factor.

The LIF signal random uncertainty, due to detector noise and laser beam mode fluctuations, was below 15% when using signal averaging of 100 pulses per line. The other error source in the absolute concentration was the uncertainty of the calibration coefficient. This factor can be isolated to the linear fit of the titration signal, where the predicted error in the slope was 2%. The iterative procedure to determine the actual H_2 quenching described above contributed another 5% to the total uncertainty. With this, the total statistical uncertainty of the H concentration measurement was less than 20%.

3.2   *Kinetic modeling*

A major motivation for implementing in situ diagnostics in reactive environments is the validation of the process models. The modeling tasks are often hampered by the scarcity of kinetic reaction data and the large uncertainties in the data that is available. This is aggravated further in surface reaction models, where experimental methods of analysis are limited. The practical modeling of the CVD diamond process must include both gas-phase and surface reaction analysis; the surface processes that determine the diamond-film growth

also have a significant impact on the gas-phase conditions close to the surface.

To verify the measured H concentration profile against numerical predictions, a one-dimensional kinetic model of the gas–surface system was built using the CHEMKIN software package with SPIN surface reaction extension. The modeled area extends to 6-mm distance from the surface; the filament was not included. The hydrogen boundary condition at the gas was taken from the absolute H concentration measurement. The hydrocarbon boundary mole fractions were introduced as a simple mixture of the major CH species, after [14]. The initial uncertainty of the gas composition is expected to settle down rapidly in the free gas, at least with regard to those species that play a significant role in the film-growth process.

The kinetic data used in the modeling was mostly taken from [15], with the following exception. As such these data predicted too high H concentrations for z values less than 1 mm. We investigated some alternative values from the literature [15–18] for those reactions that were found significant for H concentration close to the substrate, including the following surface reactions:

$$CH(s) + H \rightarrow C(s) + H_2 , \tag{2}$$
$$C(s) + H \rightarrow CH(s) \tag{3}$$

and the gas-phase reaction:

$$CH + H \rightarrow C + H_2 . \tag{4}$$

We found that the model gave the best fit to the experiment when the data for reaction (4) was taken from [17]. Table 1 presents the respective values of the Arrhenius parameters.

Figure 4 shows the measured versus modeled H vertical number density profiles at different filament temperatures.

A	β	E (kJ/mol)	Ref.
1.5×10^{14}	0	0	[15]
1.9×10^{14}	0	67000	[17]
7.9×10^{13}	0	160	[16]

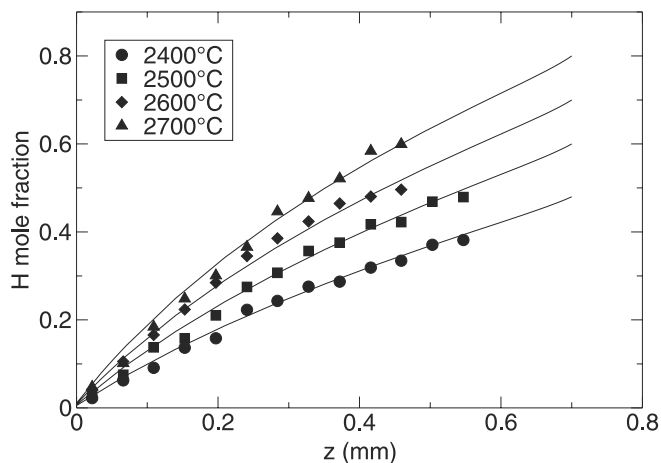**TABLE 1**   The investigated kinetic data for reaction (4)

FIGURE 4   Modeled versus experimental axial H mole fractions in the 5-wire configuration

The experimental data were obtained using the 5-wire filament, which (considering the measured lateral H profiles) close to the substrate center axis approximately produces the laterally uniform conditions that are well described by the one-dimensional model. The calculated axial gas phase mole fraction distributions show good agreement with the experiment.

The surface part of the kinetic model also includes the diamond film growth reactions that predict the growth rate. In addition to the H atom transport that is mostly determined by T_F and the filament–substrate geometry, the main factors affecting the growth rate are T_S and the input methane content. For the experimental conditions presented in this paper, the predicted diamond film growth rate was 0.9–1.4 μm/h, a typical value for a hot-filament environment with this gas composition. We have reported up to ten times higher growth rates using higher CH_4 input [9]. As noted, the LIF diagnostics could not be employed in conditions specified in this citation. We tested the model presented in [15] as such, and our corrected model for this case using 8% CH_4 input condition. The resulting growth-rate predictions were over 140 μm/h for the original model and 4.5–5.5 μm/h for the corrected model, depending on the substrate temperature. The corrected model is again in good agreement with the experimental values.

4   Conclusions

A two-dimensional two-photon measurement of H atom concentration distribution was presented. The validity of a carefully analyzed atomic H LIF concentration measurement is good in a hot-filament diamond CVD environment, and the interpretation of the signal is relatively easy, given that quenching adjustment is made under conditions with strong hydrogen dissociation.

A multi-wire filament grid was found to produce a considerably higher H concentration at the substrate surface level than a single wire. It also produced a laterally very uniform H distribution between the substrate and the filament structure. Strong and uniform H atom transport is crucial to the quality

of the diamond deposit; hence the multi-wire setup (or possibly a coiled filament) seems to be useful even with small substrate dimensions.

The validity of kinetic modeling of the diamond growth was asserted by comparison with the calibrated concentration profiles. With exploration of different cited kinetic parameters for some key reactions, the model gave predictions that agreed with the experimental results for both gas-phase concentrations and film-growth rates. This demonstrates the value of in situ diagnostics at the side of pure numerical models in the analysis of CVD and other complex reactive environments.

REFERENCES

1 T.R. Anthony: Vacuum **41**, 1356 (1990)
2 M. Frenklach, H. Wang: Phys. Rev. B **43**, 1520 (1991)
3 U. Meier, K. Kohse-Höinghaus, L. Schäfer, C.-P. Klages: Appl. Opt. **29**, 4993 (1990)
4 G. Balestrino, M. Marinelli, E. Milani, A. Paoletti, I. Pinter, A. Tebano, P. Paroli: Appl. Phys. Lett. **62**, 879 (1993)
5 K.-H. Chen, M.-C. Chuang, C.M. Penney, W.F. Banholzer: J. Appl. Phys. **71**, 1485 (1992)
6 L.L. Connell, J.W. Fleming, H.-N. Chu, D.J. Vestyck, E. Jensen, J.E. Butler: J. Appl. Phys. **78**, 3622 (1995)
7 K. Donnelly, D.P. Dowling, T.P. O'Brien, A. O'Leary, T.C. Kelly, R. Cheshire, K.F. Al-Assadi, W.G. Graham, T. Morrow, V. Kornas, V. Schultz-von der Gathen, H.F. Döbele: Diamond Relat. Mater. **4**, 324 (1995)
8 K.E. Bertagnolli, R.P. Lucht, M.N. Bui-Pham: J. Appl. Phys. **83**, 2315 (1998)
9 D.M. Li, T. Mäntylä, R. Hernberg, J. Levoska: Diamond Relat. Mater. **5**, 350 (1996)
10 J. Larjo, H. Koivikko, D. Li, R. Hernberg: Appl. Opt. **40**, 765 (2001)
11 D.G. Goodwin: J. Appl. Phys. **74**, 6888 (1993)
12 J.E.M. Goldsmith, J.A. Miller, R.J.M. Anderson, L.R. Williams: In 23rd Int. Symp. Combust. (The Combustion Institute, Pittsburgh 1990) p. 1821
13 J. Larjo, J. Walewski, R. Hernberg: Appl. Phys. B **72**, 455 (2000)
14 Y. Mankelevich, A. Rakhimov, N. Suetin: Diamond Relat. Mater. **5**, 888 (1996)
15 E. Meeks, R. Kee, D. Dandy, M. Coltrin: Combust. Flame **92**, 144 (1993)
16 A. Konnov: In 28th Int. Symp. Combust. (The Combustion Institute, Edinburgh 2000) p. 317 [data available in `http://homepages.vub.ac.be/~akonnov`]
17 B.W. Yu, S.L. Girshick: J. Appl. Phys. **75**, 3194 (1994)
18 K. Lee, M. Yang, I. Puri: Combust. Flame **92**, 419 (1993)